BeBeC-2014-30

METHODOLOGY FOR PASS-BY MEASUREMENTS ON CARS WITH BEAMFORMING

José A. Ballesteros[1], Ennes Sarradj[2], Marcos D. Fernández[1],
Thomas Geyer[2], María Jesús Ballesteros
[1]Escuela Politécnica de Cuenca, Universidad de Castilla-La Mancha
Campus Universitario, 16071, Cuenca, Spain
[2]Institut Verkehrstechnik, Brandenburgische Technische Universität Cottbus

ABSTRACT

Traffic noise is one of the most important noise sources in industrialized countries. In order to control this kind of noise, it is important to identify and to quantify the noise sources during the pass-by of a car.

Standardised methods for vehicle and tyre/road noise measurements only provide results about the time history of the sound, the sound pressure level emitted or the spectrum, but it is impossible to identify the main noise sources. Other advanced measurement methods, as sound intensity, identify the noise source but have the problem of positioning the transducers during the pass-by measurements.

In this paper, a new methodology to apply Beamforming for pass-by measurements on cars is described. To define this methodology, simulations were performed in order to design the array, the measurement scenario and to choose the beamforming algorithm most suited to process the pass-by measurement data. Once the methodology was established, it was applied to a real measurement. The results obtained were similar to other published in the literature and therefore, the applicability of the new methodology was confirmed.

1 Introduction

Traffic noise is one of the most important noise sources in industrialized countries. In the European Community the Directive 70/157/EEC establishes the regulation for homologated cars [4]. Although these limits have been reduced since 1970, traffic noise levels have not been reduced because of the increased traffic intensity and extended road/street network.

The homologation process based on an acceleration test [12] (where the car has to be fully accelerated on a test track of 20 m length) has forced vehicle manufacturers to reduce engine and intake/exhaust noise. These sources are strongly engine-load-dependent and thus dominate the low-speed, high-load acceleration test. However, the process has had less impact on tyre noise and on the noise caused by vehicles at speed much in excess of 50 km/h [9]. The noise reductions in the engine and intake/exhaust have made the tyre/road noise the main noise source to be reduced.

Taking into account that the main noise source in the cities is the traffic and that the homologation tests are performed in movement, apart from the global pass-by noise, it is also important to identify and to quantify the noise sources that take place during the pass-by of a car.

The literature shows two ways for pass-by measurements. Among the standardised methods it is possible to highlight the Coast-By method [11], the Close-Proximity method [10], the laboratory Drum method [13], the Trailer Coast-By method [11] or the Acceleration Pass-By method (ISO 362 [12]). Nevertheless, these methods only provide results about the time history of the sound, the sound pressure level emitted or the spectrum, but it is impossible to identify the main noise sources. Moreover, one finds advanced measurement methods based on Laser Doppler Vibrometry [17], Source Height Measurement [8], Sound Intensity [5], Nearfield Acoustic Holography [19] or Spatial Transformation of Sound Fields [7]. These methods identify the noise source but have the problem of positioning and fixing the transducers during the pass-by measurements.

Another possible method to obtain information on the position and strength of noise sources is the Beamforming. The Beamforming technique for moving sources has been used for noise source identification in airplanes or trains [15]. This technique was also applied in cars but only in very few cases.

There is no standardization for pass-by measurements in cars with Beamforming. In each research project [3, 14, 16, 18] different microphone array configurations and measurement scenarios are used. The distance from the array to the car and the array size are not uniform. There are studies in which the car is driven at constant speed and others where it is driven in acceleration according to the ISO 362 requirements [12]. In this paper, a methodology for pass-by measurements on cars is defined and analyzed through simulations. Once the measurement scenario is defined, the results from a real measurement are compared with the results from other techniques found in the literature.

2 Beamforming Algorithms

Beamforming can either be formulated in the time domain (the signals are delayed and summed) or in the frequency domain (the cross-spectral matrix of the microphone signals is multiplied by a steering vector). Static measurements are usually treated in the frequency domain, although the results obtained in time domain should be equal. Measurements with a source in motion relative to the microphone array can only be treated in the time domain. In these cases, the frequency perceived by each microphone is continuously changing with the time due to the Doppler effect; therefore, no correlation at the same frequency can be built between the different microphone signals [6].

Fixed focus and moving focus algorithms are chosen to process the data. The main difference between them is that, in the first case, the focus of the array is spatially fixed [6]. In the second one, the focus is following the trajectory of the noise source [21].

The method presented in [6] for the fixed focus algorithm is a hybrid one: the beamforming results are calculated in the time domain and the point spread function is approximated in the frequency domain taking into account an average Doppler frequency shift. The ideal way to solve the deconvolution problem would be to compute the point spread functions in the time domain and minimize the cost function over all the frequency lines simultaneously. As the calculation of the point spread functions in the time domain for the whole scanning area is alone not affordable in terms of computing time, Guérin [6] proposed an alternative calculus of the point spread function where an average Doppler frequency shift calculated between the centre of the focusing domain and the array centre is introduced.

The basic idea of the moving focus algorithm is to focus on an assumed source position and to apply a signal processing to microphone signals, such that an output is generated that meets two important conditions. First, if the assumed source position is the actual position of the source, the output should be the source signal itself, possibly scaled by some known factor. Second, if the source is at any other location, the output should be minimal and in any case its amplitude less than that of the source signal. With these properties the beamformer is a directional sound receiver with true three-dimensional directivity characteristic. The typical application is to steer the beamformer consecutively to several assumed source positions with a regular grid. From the outputs, a map of sound sources (Beamforming map) is constructed [21].

3 Simulation

A simulation is done to choose the array layout (microphone arrangement in the array) most suited for the desired measurements and the best algorithm to process the data.

To carry out the simulation, a car composed of six point noise sources emitting random and incoherent noise is simulated. These noise sources simulate the engine noise, the tyre/road noise and the exhaust noise. Their locations are shown in blue in figure 1.

In figure 2 the scenario used for the simulation is shown. A distance between the array and the car of 5 m and a 14 m linear trajectory of the car are defined. Knowing that the array aperture angle should be less than 90^o, and since the distance between the array and the car is 5 m, the maximum length of the pass-by is 10 m. To avoid the results being influenced by the length of the trajectory, the chosen length is defined longer than the maximum length to evaluate. This trajectory is traversed by the six point noise sources that define the car at a speed of 50 km/h.

The resolution is defined as the smallest distance between two possible separate monopole

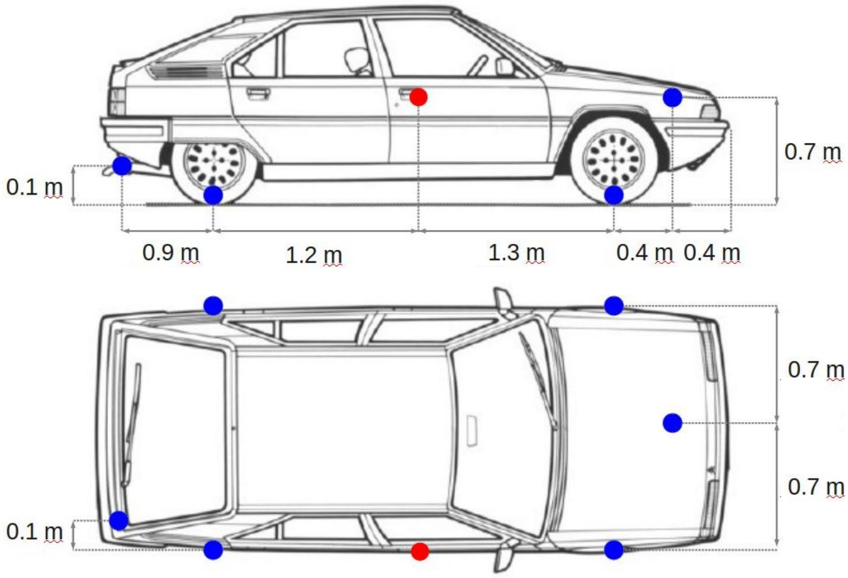

Figure 1: Location of the noise sources (blue) and the reference point for the array (red).

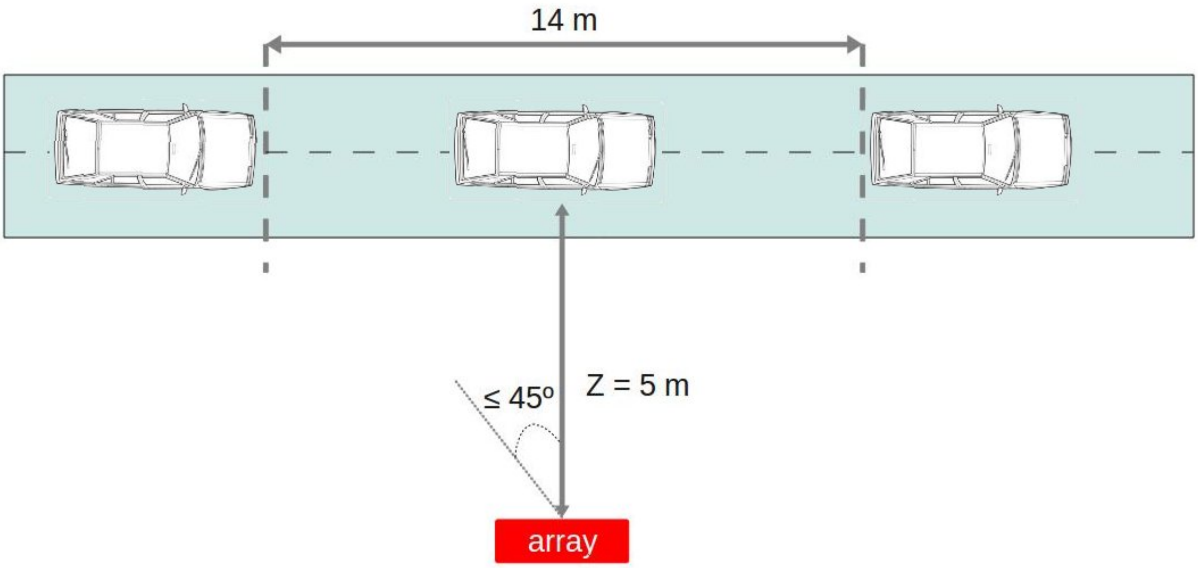

Figure 2: Simulation scenario.

source positions in a source map. For Beamforming the near-axial resolution is roughly:

$$R = 1.22\frac{Z}{D}\lambda \tag{1}$$

where Z is the measurement distance, D is the array diameter and λ is the wavelength [2].

As the resolution is proportional to the wavelength, it is often not acceptable at low frequencies, thus usually requiring that the Beamforming results are meaningful for frequencies above approximately 1 kHz. Taking both this insufficient resolution at very low frequencies as well as the fact that the noise emission from cars is usually higher at low frequencies into account, only the third octave bands centered on 500, 1000 and 2000 Hz were chosen for the simulation. It can be assumed that the algorithm that provides good results at these frequencies will most probably also deliver satisfying results at higher frequencies.

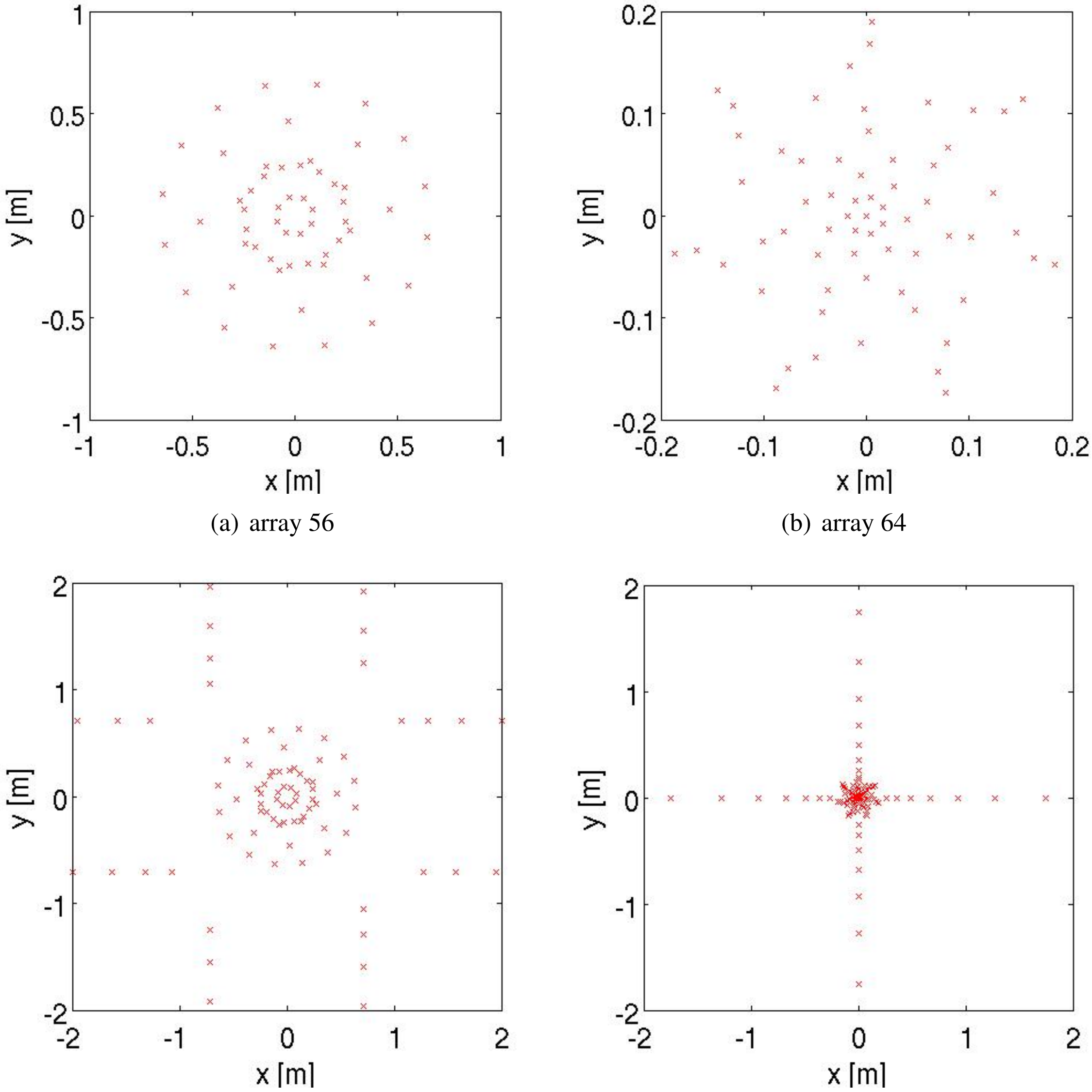

(a) array 56 (b) array 64

(c) array 84 (d) array 92

Figure 3: Initial layout for the arrays.

Initially, two planar arrays of 56 and 64 microphones, respectively, were chosen (figure 3 (a) and (b)). The number of microphones of these arrays can be increased with 28 additional microphones, located on some external arms attached to the center array, obtaining an 84-microphone array and a 92-microphone array, whose initial layouts are shown in figure 3 (c) and (d)).

Figures 4 and 5 show, for the fixed focus and moving focus algorithm respectively, the results of the simulations for the time point when the simulated car is approximately in front of the array. It was observed that the 56-microphones array produces the best results due to its larger aperture, with a better separation of the noise sources. When the additional arms were used, the noise source separation was improved, because the aperture is further increased. Therefore, the 84-microphone array shown in Figure 3 (c) was chosen for the present study.

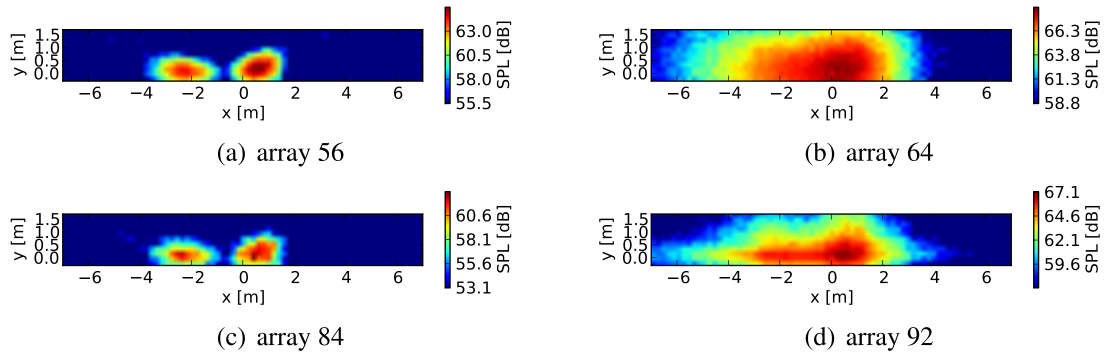

(a) array 56 (b) array 64

(c) array 84 (d) array 92

Figure 4: Results in the third octave band of 2 kHz with fixed focus algorithm.

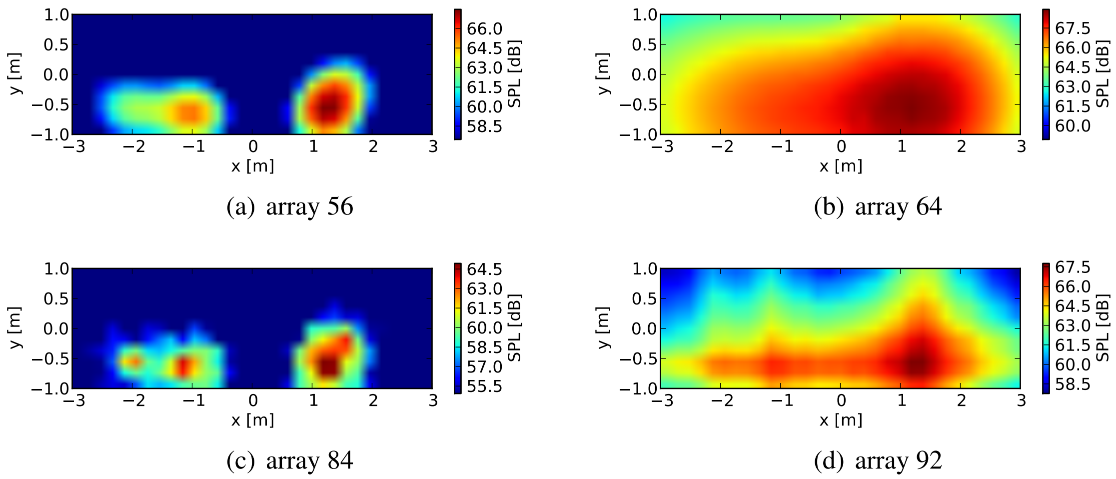

(a) array 56 (b) array 64

(c) array 84 (d) array 92

Figure 5: Results in the third octave band of 2 kHz with moving focus algorithm.

To obtain the best results possible, different configurations of the arms of the 56-microphones array are simulated. These configurations are shown in figure 6. The results are very similar in all the cases, but those obtained with the *array 84_2* (figure 6 (c)) are better. Therefore, it is chosen to perform the measurements.

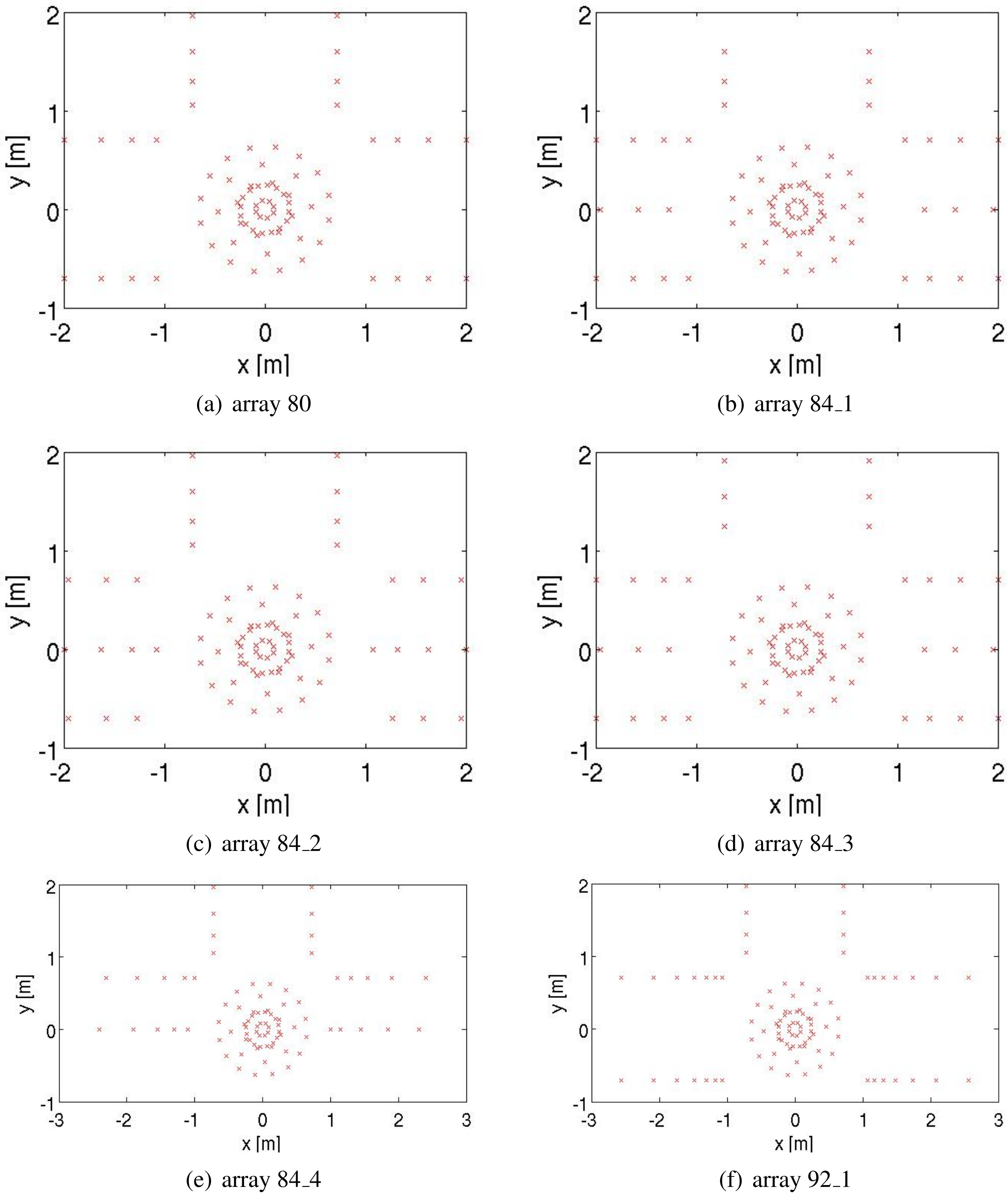

Figure 6: Different configurations for the arms of the 56-microphones array.

Figure 7 and 8 show the results obtained for the *array 84_2* in the third octave band of

2 kHz with fixed focus algorithm and moving focus algorithm respectively. The noise source maps show (from left to right and from top to bottom) the noise sources visibles when the simulated car is in different points of the trajectory, being 0.93 m the distance traversed by the car between each map and the following.

The results for the fixed focus algorithm (figure 7) show that when the simulated car is in front of the array (point 0 in the maps), it is possible to observe two noise sources that correspond with the noise sources of the front axle of the car and the noise sources of the rear one. Nevertheless, when the car is at the beginning or at the end of the trajectory, this algorithm cannot separate the different noise sources, that appear as a linear noise source.

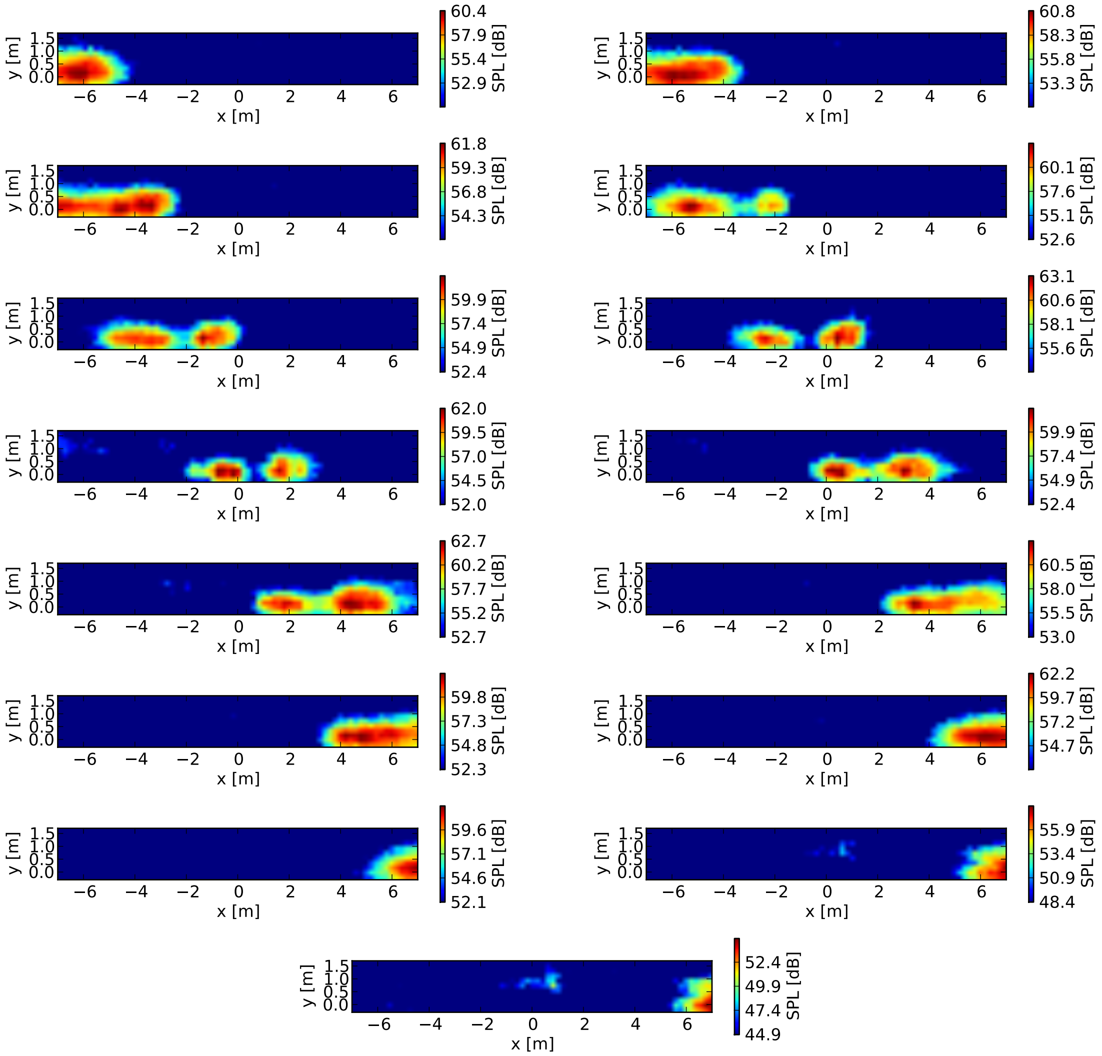

Figure 7: Results in the third octave band of 2 kHz for the array 84_2 with fixed focus algorithm. Details of the maps are given in the text.

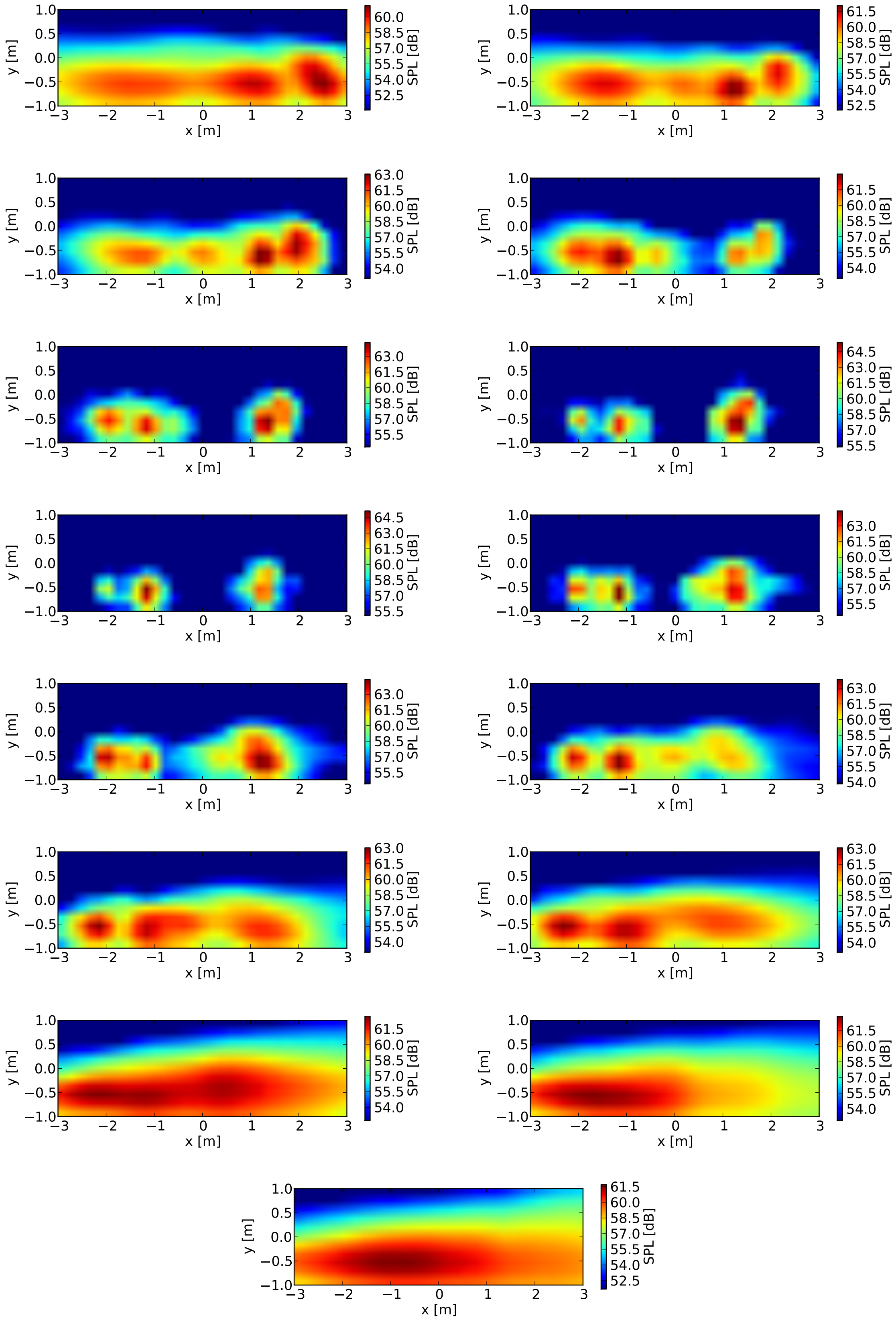

Figure 8: Results in the third octave band of 2 kHz for the array 84_2 with moving focus algorithm. Details of the maps are given in the text.

In figure 8, the results in the third octave band of 2 kHz from the chosen array with the moving focus algorithm are shown. When the car is at the beginning and at the end of the trajectory, the noise sources are shown as a linear source due to the angle of the array focus. On the other hand, when the car is near the array, a clear separation of the noise sources located at the tyres can be observed. In some cases, the engine noise source can also be observed, although this source appears to be connected to the noise sources at the front tyres in almost all cases.

Due to the differences stated above, the moving focus algorithm is chosen to process the measurement data, because it obtains better separation of the noise sources, as can be observed from a comparison between figures 7 and 8.

To define the optimum height of the array (distance of the center of the array from the ground) that allows the separation of the noise source and its image source, another simulation is done. In this case, two coherent noise sources equidistant 0.5 m from the ground are defined as it is shown in figure 9. These two sources follow the same trajectory that was defined in the previous case at a speed of 50 km/h. For the simulation, three different array heights were tested: 1 m, 1.5 m and 2 m.

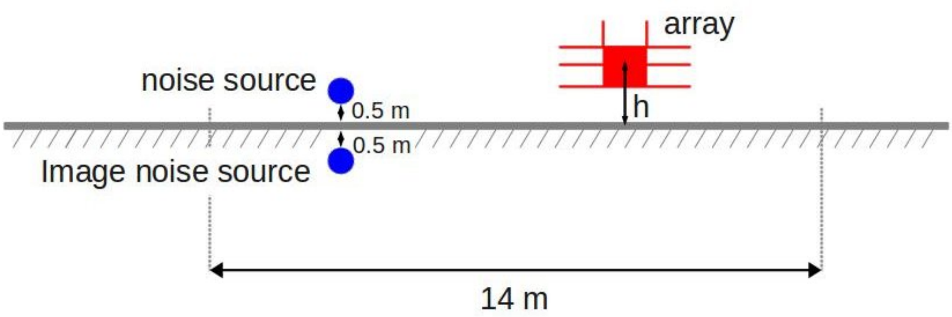

Figure 9: Noise source separation scenario (h is the array height).

Taking into account that the differences observed among all the simulations were very small, a height of 1.5 m from the ground to the center of the array was chosen. Figure 10 shows the results obtained for moving focus algorithm at 2000 Hz, where each map shows (from left to right and from top to bottom) the location of the noise sources at different points of the trajectory, being 0.93 m the distance traversed by the sources between each map and the following. It is observed how only the two sources are not separated at the end of the trajectory, obtaining a very good separation when the two sources are in front of the array.

4 Application in a Real Measurement

4.1 Measurement Setup

To carry out the measurements, a similar setup like the one used for the simulations was chosen. This setup is shown in figure 11. The main difference is that the lenght of the measurement

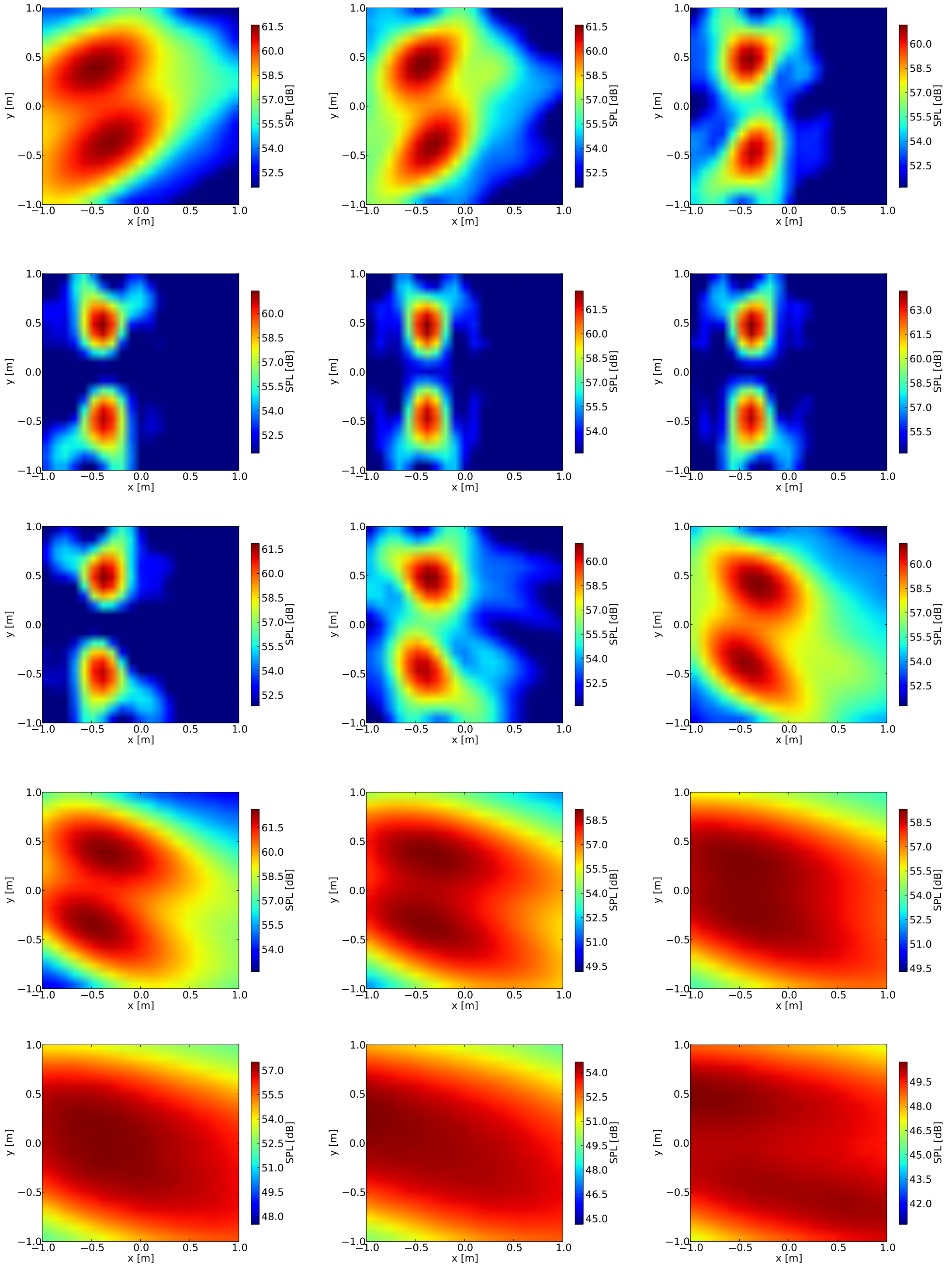

Figure 10: Results for the third octave band of 2 kHz with moving focus algorithm for h=1.5 m.

area was restricted to 10 m, which is the maximum lenght for the aperture angle of the array, as it was explained in section 3.

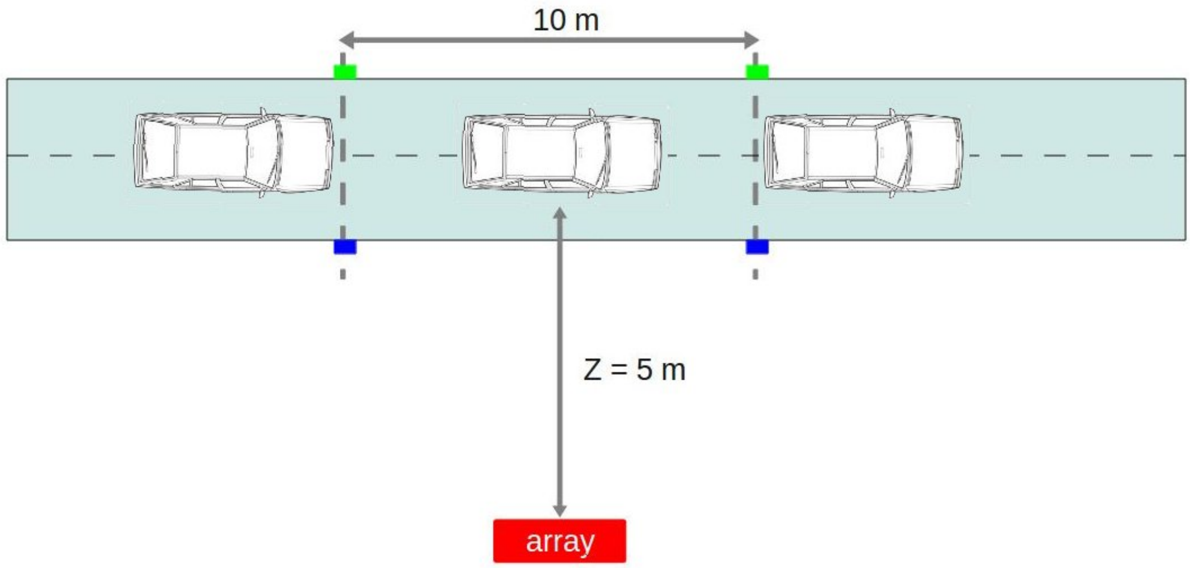

Figure 11: Measurement setup.

The measurement length was defined by two lightbarriers from the Brüel and Kjaer pass-by noise measurement system. These lightbarriers were connected to a detector emitting a trigger signal to start and stop the measurement. When the car went into the measurement area, the first lightbarrier was activated, and the measurement started; 5 m after the activation of the second lightbarrier the measurement was stopped, in other words, when the whole car crossed the measurement area. The end of the measurement was determined calculating the time spent by the car to traverse 5 m at the speed of the pass-by. Figure 12 shows the array and the locations of the lightbarriers (green and blue squares) for the measurements.

To carry out the tests, a medium-sized car from the year 2009 with a gasoline engine was chosen with 195/65 R15 91H tyres. The pass-by tests were performed at constant speed in the measurement area, as has been proposed in the revision to the ISO 362 standard [1]. To minimize the engine influence, the pass-bys were done at 80 km/h in 6^{th} gear. During the measurements, the wind speed was not too high (1.7 m/s), the temperature was 24.1°C and there was no rain or snow. The measurement process is shown in figure 13.

4.2 Processing Setup

The data obtained from the measurements were processed with a moving focus algorithm because it provided the best results (section 3). Nevertheless, to improve the noise source location maps obtained in the simulations, with a more precise source localization and less

Figure 12: Equipment location for the measurements.

Figure 13: Measurements process.

sidelobes in the map, a little change was done to process the data.

Instead of performing beamforming on the trajectory of the complete drive-by (10 m), the distance was splitted in subsequent blocks, using a grid with a small extent in the direction of travel and using a very short trajectory for Beamforming with that grid. Then, a new set of samples was taken, being it delayed the time the car needs to travel a distance equal to the grid increment using the same trajectory for Beamforming. This process was repeated in succession.

The maps from each set of samples were then averaged, each grid increment offset to give a long overall map. In this way, the array has the best resolution and has nearly the same properties for each map that is averaged. The one grid increment distance helps preventing vertical stripes that may occur otherwise.

From the maps for each third octave band, the sound pressure of each tyre is calculated using the sound power integration technique [22] over appropriate sectors. The sectors used in the present study were centered at the tyre center in the x-direction and had a length of 1.5 m. In the y-direction, the sectors extended from the ground to 1 m above the ground. The sectors chosen can be observed in figure 14. Once that the sound pressure for each frequency band was obtained, the spectrum of each tyre was calculated.

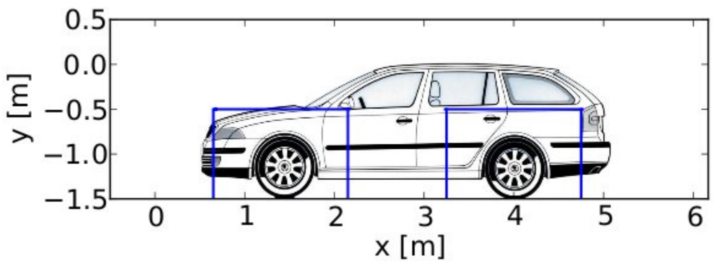

Figure 14: Sector definition.

4.3 Results

In figure 15 the results for both, the front and the rear tyre of the car at 80 km/h are shown. The basic trends of the sound pressure level spectra are similar and independent of the tyre. These trends show a peak around 1 kHz and a decrease of the sound pressure level from that peak with increasing frequency.

Figure 16 shows the noise source map at 80 km/h. It can be seen by the noise source location that at low frequencies the area covered by the source is larger. Not only because the noise source characteristics are different at these frequencies, but also due to the smaller resolution of the Beamforming algorithm [2]. When the frequency is increased, the noise source is focused on the contact path between the tyre and the road near the center of the tread. The emission from the front tyre is higher than from the rear.

In [20] a wide review of tyre/road noise is discussed. The results included in this work show a typical spectrum with a peak around 800 Hz – 1 kHz due to a multitude of coinciding factors: tyre tread patterns, pipe resonances in longitudinal grooves, lateral grooves, Helmholtz resonance, tangential resonances in tread block elements, belt resonance or the horn effect.

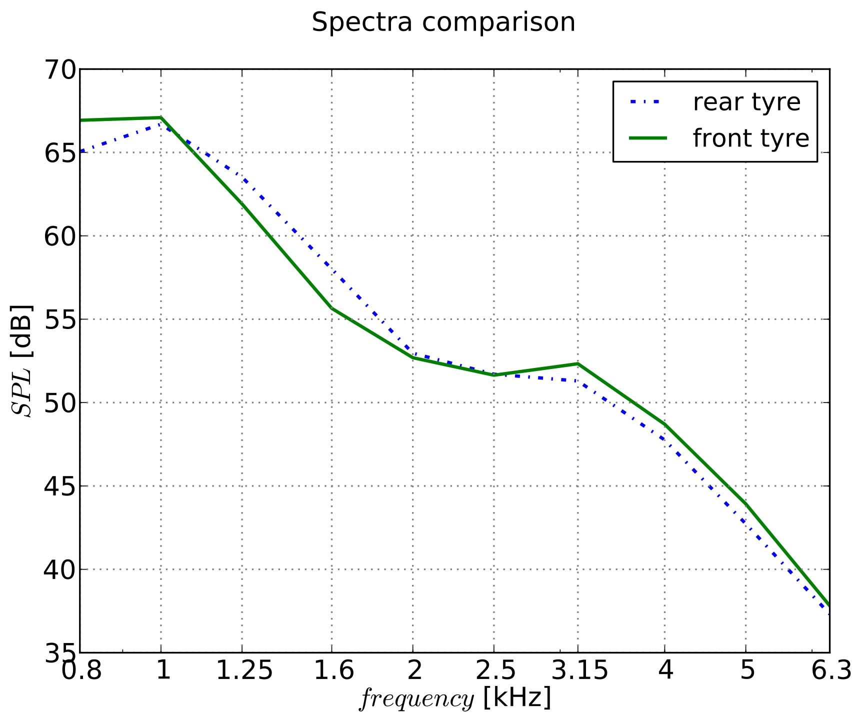

Figure 15: Spectra comparison.

Regarding the noise source locations in tyre/road noise, some studies are also given in [20]. In these studies, different techniques applying sound intensity measurements, vibrations measurements, near-field acoustic holography and spatial transformation of the sound fields are used. The conclusions exposed in that work show that the noise sources are located very close to the leading and trailing edges of the tyre, most prominently near the center of the tread and that the emission from the front of the tyre is slightly higher than from the rear.

If the conclusions shown in [20] are compared with the present results, it is possible to see that there is a high correlation between them. Thus, it is possible to say that the methodology proposed in this paper delivers useful results for this kind of measurements.

5 Conclusion

Although the Beamforming for moving sources is applied successfully to locate and to analyze noise sources at airplanes and trains, there are only a few papers where this technique is applied to cars. The present paper deals with the methodology that is neccessary to perform pass-by measurements on cars using microphone array technique and beamforming algorithms.

In a first step, simulations were performed to determine the parameters required to carry out the intended measurements. Based on the results from the simulations, a 56-microphone array with 28 additional microphones, located on 8 external arms attached to the center array, was chosen because it obtained better noise source separation than other arrays evaluated. This

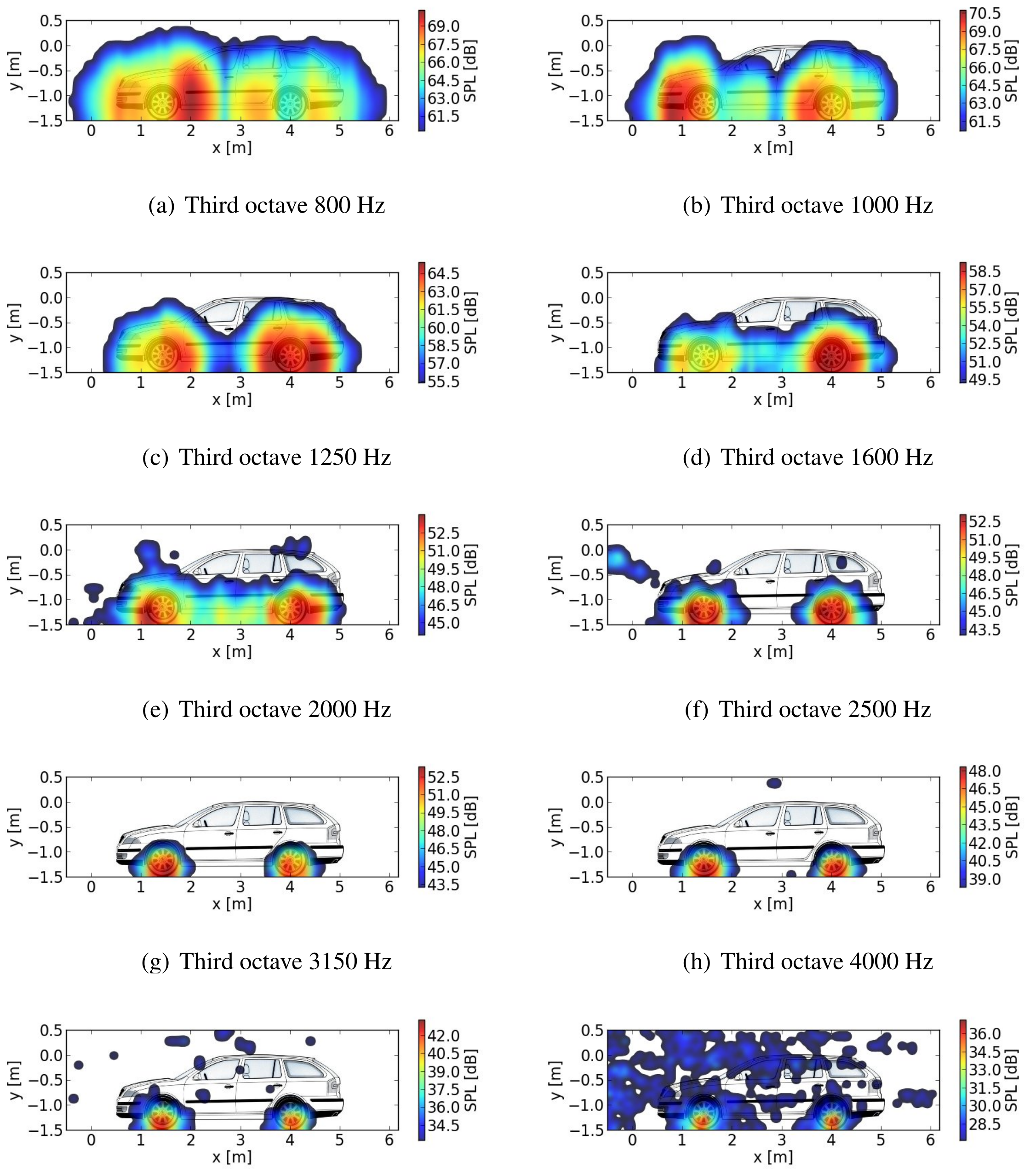

(a) Third octave 800 Hz (b) Third octave 1000 Hz

(c) Third octave 1250 Hz (d) Third octave 1600 Hz

(e) Third octave 2000 Hz (f) Third octave 2500 Hz

(g) Third octave 3150 Hz (h) Third octave 4000 Hz

(i) Third octave 5000 Hz (j) Third octave 6300 Hz

Figure 16: Noise mapping at 80 km/h.

array should be located at a distance of 5 m of the pass-by line, with a vertical distance of 1.5 m between the center of the array and the gound in order to separate the noise source from its image source. To process the data obtained from the measurements a moving focus algorithm was chosen, as it obtained better noise source separation than the fixed focus algorithm.

The evaluation of the spectra showed a common spectrum trend independent from the tyre. This trend consists of a peak around 1 kHz with a decrease of the sound pressure level when the frequency is increased.

Through the noise source maps the location of the noise source was calculated in the pass-by of the car near the center of the tread, identifying also higher emission from the front of the tyre than from the rear.

A comparison between the results from the present study with those from other researches found in the literature shows a good agreement. Thus, it is possible to conclude that the methodology proposed is suitable for noise source identification during the pass-by of cars.

References

[1] M. Braun, S. Walsh, J. Horner, and R. Chuter. “Noise source characteristics in the iso 362 vehicle pass-by noise test: Literature review.” *Applied Acoustics*, 74(11), 1241–1265, 2013.

[2] J. Christensen and J. Hald. “Technical review, beamforming.” *Bruël & Kjær*, 1, 2004.

[3] A. Crewe, F. Perrin, V. Benoit, and K. Haddad. “Real-time pass-by noise source identification using a beam-forming approach.” *Society of Automotive Engineers, 400 Commonwealth Dr, Warrendale, PA, 15096, USA*, 2002.

[4] European Commission. “Directive 70/157/EEC of 6 February 1970 on the approximation of the laws of the Member States relating to the permissible sound level and the exhaust system of motor vehicles.” 1970.

[5] General Motors. “Road tire noise evaluation procedure.” *test Procedure GMN7079TP*, 2004.

[6] S. Guérin, C. Weckmüller, and U. Michel. “Beamforming and deconvolution for aerodynamic sound sources in motion.” In *1st Berlin Beamforming Conference*, pages 21–22. 2006.

[7] J. Hald. “Use of spatial transformation of sound fields (STSF) techniques in the automotive industry.” *Technical Review*, (1-1995), 1995.

[8] J.-F. Hamet, M.-A. Pallas, D. Gaulin, and M. Bérengier. “Acoustic modelling of road vehicles for traffic noise prediction: determination of the source heights.” *Proc. of the 16th ICA, Seattle, USA*, 1998.

[9] M. Harrison. *Vehicle refinement: controlling noise and vibration in road vehicles*. Elsevier Butterworth-Heinemann, 2004.

[10] ISO 11819-2. “Acoustic - Method for measuring the influence of road surfaces on traffic noise - Part 2: “The Close Proximity Method”.” (ISO 11819-2), 2000.

[11] ISO 13325. "Tyres – Coast-by methods for measurement of tyre-to-road sound emission." (ISO 13325), 2003.

[12] ISO 362. "Measurement of noise emitted by accelerating road vehicles." (ISO 362), 2009.

[13] JASO C606-81. "Test procedures for tire noise." (JASO C606-81), 1981.

[14] H. Kook, G. Moebs, P. Davies, and J. Bolton. "An efficient procedure for visualizing the sound field radiated by vehicles during standardized passby tests." *Journal of Sound and Vibration*, 233(1), 137–156, 2000.

[15] U. Michel. "History of acoustic beamforming." *BeBeC*, 2006.

[16] U. Michel, B. Barsikow, P. Böhning, and M. Hellmig. "Localisation of moving sound sources with phased microphone arrays." In *Inter-Noise 2004, Prague, Czech Republic, 22.- 25 August 2004*. 2004.

[17] Ometron. "Areas of vibrometer applications." `http://www.ometron.com/applications/index.html`, 2012. Accessed January 30, 2014.

[18] D. Püschel, M. Auerbach, and W. Bartolomaeus. "Pass-by measurements using array techniques." In *EURONOISE 2009, Edinburgh, Scotland, 26-28 October 2009*. 2009.

[19] R. J. Ruhala and C. B. Burroughs. "Localization of tire/pavement noise source regions." *Noise Control Engineering Journal*, 56(5), 318–331, 2008.

[20] U. Sandberg and J. A. Ejsmont. *Tyre/road noise reference book*, volume 59040. Informex Kisa, Sweden, 2002.

[21] E. Sarradj, C. Fritzsche, and T. Geyer. "Silent owl flight: bird flyover noise measurements." *AIAA journal*, 49(4), 769–779, 2011.

[22] P. Sijtsma and R. W. Stoker. "Determination of absolute contributions of aircraft noise components using fly-over array measurements." *AIAA paper*, 2958(2004), 10, 2004.